Analytical model of propagating sand ripples

R. B. Hoyle
Department of Applied Mathematics and Theoretical Physics, University of Cambridge, Cambridge CB3 9EW, United Kingdom

A. W. Woods
School of Mathematics, University of Bristol, Bristol BS8 1TW, United Kingdom

(Received 21 April 1997)

We formulate a simple phenomenological model of aeolian sand ripple migration based upon a balance between grain hopping driven by saltation and grain rolling or avalanching under gravity. We develop a set of model equations governing the evolution of the ripple slope. The model has solutions describing steadily propagating isolated ripples, produced by a horizontal saltation flux, and periodic trains of ripples, which develop when the saltation flux is inclined to the horizontal. In the case of an inclined saltation flux, the ripple wavelength is controlled by the length of the shadow zone, as suggested by R. P. Sharp [J. Geol. **71**, 617 (1963)]. Although very simple, our model predicts some of the qualitative features shown by sand ripples in experimental or field studies [R. A. Bagnold, *The Physics of Blown Sand and Desert Dunes* (Methuen and Co., London, 1941); R. P. Sharp, J. Geol. **71**, 617 (1963)]. We find that ripples only develop above a certain threshold value of the saltation flux intensity. Furthermore, at relatively low saltation fluxes, the lee slope of the ripple is a smooth curve, whereas above a critical value of the saltation flux, a slip face develops near the crest. The model predicts a decrease in the speed of propagation as the ripple becomes larger, consistent with observations that smaller ripples are eliminated by ripple merger [R. P. Sharp, J. Geol. **71**, 617 (1963)], and also with numerical simulations [R. S. Anderson, Earth-Sci. Rev. **29**, 77 (1990); S. B. Forrest and P. K. Haff, Science **255**, 1240 (1992); W. Landry and B. T. Werner, Physica D **77**, 238 (1994)].
[S1063-651X(97)05911-4]

PACS number(s): 81.05.Rm

I. INTRODUCTION

As the wind blows across a loosely packed sand bed, the sand tends to be organised into propagating waves known as aeolian sand ripples. These ripples, which occur both in the desert and at the seashore, are small, with a wavelength of a few centimetres, and with heights roughly one-fifteenth or one-twentieth of their wavelength. Their crests lie perpendicular to the direction of the wind.

Bagnold [1] presented a model of the formation of aeolian sand ripples based upon the concept of energetic saltating grains impacting the ripple and causing displacement of the grains in the ripple. The displaced grains then hop up the stoss (windward) slope of the ripple, and it is this that causes the ripple to propagate. The saltating grains are assumed to be entrained from the sand bed upwind and to be sufficiently energetic that they continue downwind of the ripple. This saltation process is illustrated in Fig. 1, which also shows a typical aeolian sand ripple and explains the terminology used to refer to different parts of the ripple. Bagnold's early work on sand ripple formation has been developed and modified by subsequent workers, e.g., Anderson [2,3], and compared

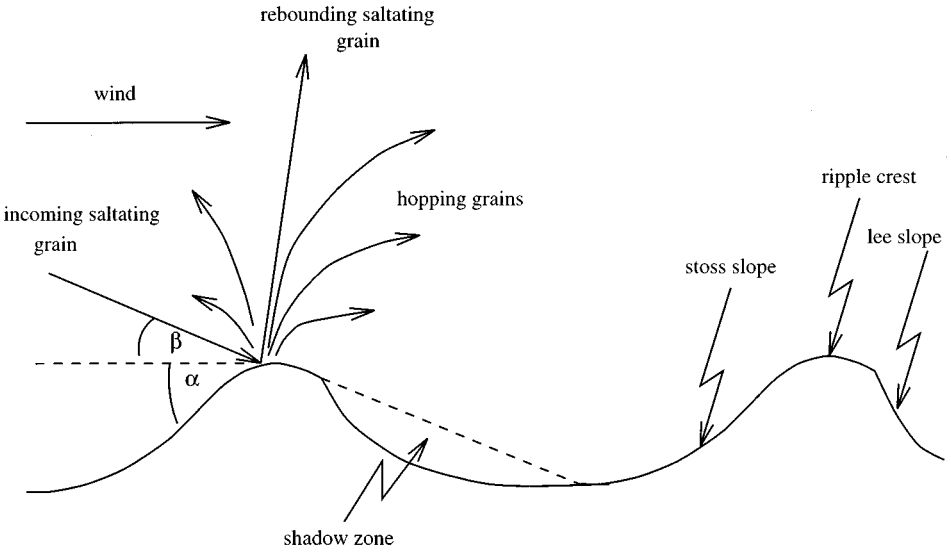

FIG. 1. A schematic diagram to show the stoss and lee slopes, the ripple crest, and the shadow zone. The saltating particles travel in the direction of the wind and impact the bed at an angle α. The impacting grain rebounds, and knocks several other grains out of the bed, causing them to hop along the surface.

with field observations, for example, Sharp [4], and numerical experiments, for example, Anderson [3], Nishimori and Ouchi [5], and Landry and Werner [6].

Much recent analytical and experimental work has focused on the microscopic details of grain migration along the ripple. The hopping of the displaced grains has been studied by Ungar & Haff [7], Mitha *et al.* [8] and Anderson [2]. Anderson [2] used this information to produce a theoretical model of the initial generation of ripples from a flat bed. The deposition of sand grains on the lee slope of sand dunes, which leads to oversteepening and avalanching, was studied by Hunter [9] and Anderson [10]. This work suggests constraints on the ripple slope.

Both Bagnold [1] and Sharp [4] made field observations of sand ripple motion and interaction. Sharp [4] found that the stoss slope angle has a maximum inclination in the range $8°-10°$, which does not vary significantly with ripple size. This is in accord with the theoretical prediction [11] that the process of saltation becomes energetically inefficient if the angle of impact exceeds 15°. Rumpel [11] predicted that it is impossible to maintain a constant population of saltating grains when the surface is tilted by more than 15° against the incoming sand flux. He suggested that the stoss face is built up by saltation until it is at an angle of 15° to the incoming flux, when saltation becomes subdued. This suggests that if the saltation flux is at an angle β to the horizontal, then the maximum steepening of the stoss face is $15°-\beta$. Bagnold [1] observed that the lee slope never exceeds an initial angle of about 34°. This is in accord with theoretical work showing that the deposition of grains on the lee slope of sand dunes leads to oversteepening and avalanching [9,10]. Avalanching maintains the lee slope at an angle of around 32°–34° [12] near the ripple crest. Aeolian sand ripples show a similar feature: Sharp [4] observed that the lee slope of a sand ripple is composed of a short straight slope near the crest, inclined at an angle of about 30° to the horizontal, followed by a longer and shallower, concave slope.

Other field observations suggest that ripple wavelength tends to increase with time by ripple merger [4], and that longer waves are taller [13,4]. Sharp argued that the ripple wavelength is determined by the length of its shadow zone, that is, the region of the lee slope that is shielded from the saltation flux by the ripple crest. He also suggested that larger ripples would move more slowly than small ones. Furthermore, he conjectured that at low wind speeds, the stoss slope would be much longer than the lee, but that increasing wind speed should lead to a greater degree of symmetry.

In recent numerical experiments, Anderson [3], Forrest and Haff [14], and Landry and Werner [6] have investigated the macroscopic motion of sand ripples by computer simulation, in which individual grains are followed as they interact with each other. Some of the numerical results show similar features to the observations described above. In particular, ripple speed is found to vary inversely with height, so that small ripples catch up with larger ones and merge into them. This is consistent with Sharp's observation that smaller ripples are eliminated by merger. Nishimori and Ouchi [5] use a similar technique to investigate both small and large scale features in three dimensions, and produce convincing contour plots of simulated sand ripples and barchan dunes. They also find a threshold wind force for the development of ripples. Anderson and Bunas [15] investigated the effects of different grain sizes numerically using a cellular automata approach. They found that the differential motion of small and large grains can lead to reverse grading in the ripples.

The purpose of the present contribution is to develop a framework within which analytical models of the macroscopic motion of sand ripples may be developed, following the work of Anderson [2]. The current work is an extension of Hoyle [16]. We develop some simple phenomenological models of saltation, hopping, rolling, and avalanching, which account for the observations described above, and consider how a combination of these processes might determine ripple shape and migration. We derive a set of model equations governing the evolution of the ripple slope. The theory enables us to predict some qualitative changes in the structure of the ripples with size and strength of the saltation flux. First we consider a horizontal saltating flux, and present solutions that describe isolated ripples. Next, we allow the saltation flux to be inclined to the horizontal, and predict that this leads to the formation of a periodic train of ripples. We show that in our model, as the intensity of the saltation increases, the lee face of the ripple steepens and eventually develops a slip face. This provides a natural distinction between subcritical ripples characterized by a smooth, curving lee slope, and supercritical ripples, which include a slip face on the lee slope.

II. PROCESSES GOVERNING SAND RIPPLE DEVELOPMENT

A. Hopping

Aeolian sand ripples are formed by the action of saltating sand grains on surface roughness. In saltation, grains are whipped along the surface of the sand bed by the wind, impacting the bed at small angles to the surface, typically 10°–16° [1], and with high speed (of order $\leqslant 1$ m/s, [15]). Despite the gusting of the wind, the impact angle appears to remain fairly constant. The saltating grains rebound at slightly higher angles, but still with high speed, and it is assumed for the purposes of this model that these grains are sufficiently energetic that they do not fall onto the ripple surface, but continue in saltation. The impacts lead to the ejection of sand grains from the bed. The ejected grains, which have much lower speeds than the saltating grains, hop along the surface of the ripple; they are said to be in ''reptation'' [8]. Typically, the distance a reptating particle hops is much less than one ripple wavelength [1], and recent modeling suggests therefore that reptating particles have an important role in ripple formation.

For simplicity we restrict our attention to two-dimensional ripples whose surface remains of small inclination, no greater than 34°, consistent with observations [1,4]. Also, we assume that the number, $N(x,t)$, of sand grains ejected per unit time, per unit surface length, from the surface at a position x along the ripple, at time t, is proportional to the flux of saltating grains perpendicular to the surface at that point:

$$N(x,t) = J \sin(\alpha+\beta), \tag{1}$$

where α is the slope of the surface, β is the angle of impact that the saltation flux makes with the horizontal, and J is a

constant of proportionality. We assume that each sand grain ejected from the surface hops a horizontal distance a, with probability $p(a)$, where

$$\int_{-\infty}^{\infty} p(a)da = 1, \tag{2}$$

and define the mean hop length $\overline{a}$, as

$$\overline{a} = \int_{-\infty}^{\infty} ap(a)da. \tag{3}$$

We shall assume that $\overline{a} > 0$. Thus the net displacement of the sand is in the direction of the saltating flux, in accordance with observations. The probability distribution $p(a)$ contains all the information about the transfer of momentum from the saltating particles to the reptating particles. In practice, this must be determined experimentally. For example, Ungar and Haff [7] described the variation in hop lengths using a ''splash'' function, and Mitha *et al.* [8] measured the distribution of hop lengths for a bed of steel ball bearings. In the present analysis, we therefore assume that $p(a)$ is known.

Then the net number $\delta n(x,t)$ of sand grains arriving between positions x and $x+\delta x$, in time δt, is the difference between the number hopping in and the number hopping out,

$$\delta n(x,t) = \left\{ -\int_{-\infty}^{\infty} p(a)[N(x,t) - N(x-a,t)]da \right\} \delta x \, \delta t. \tag{4}$$

The change δy in the surface elevation $y(x,t)$ in time δt, is given in terms of the change in the cross-sectional area of the ripple by

$$\delta x \, \delta y(x,t) = a_p \delta n(x,t), \tag{5}$$

where a_p is the average cross-sectional area occupied by a sand grain in the ripple. Combining the last two equations leads to an equation for the evolution of the surface elevation,

$$\frac{\partial y}{\partial t}(x,t) = -a_p \int_{-\infty}^{\infty} p(a)[N(x,t) - N(x-a,t)]da. \tag{6}$$

We now introduce a number of approximations that simplify the analysis and that are generally valid for sand ripples. Typically, the hop length is short compared to a wavelength [1], so we can expand the integrand in Eq. (6) as a Taylor series in a. We also assume that the slope of the ripple, and hence the gradient $N(x,t)$, varies slowly, except at the troughs and crests, as suggested by observations [1,4], so that we may truncate this Taylor series at first order [3,14]. Specifically, we require

$$\frac{\partial^2 N}{\partial x^2}(x,t) \int a^2 p(a)da \ll \frac{\partial N}{\partial x}(x,t) \int ap(a)da \tag{7}$$

for this truncation to be valid. In this case, we can simplify Eq. (6) to the form

$$\frac{\partial y}{\partial t}(x,t) = -a_p \int ap(a) \frac{\partial N}{\partial x}(x,t)da = -a_p \overline{a} \frac{\partial N}{\partial x}(x,t). \tag{8}$$

Noting that the angle of slope of the surface, α, may be expressed as

$$\alpha = \tan^{-1}(\partial y/\partial x), \tag{9}$$

we may rewrite the definition (1) in the form

$$N(x,t) = J \sin(\alpha+\beta) = J \sin\{\tan^{-1}(\partial y/\partial x) + \beta\}$$
$$= \frac{J\{(\partial y/\partial x)\cos\beta + \sin\beta\}}{[1+(\partial y/\partial x)^2]^{1/2}}. \tag{10}$$

We may combine this with Eq. (8) to obtain the equation

$$\frac{\partial y}{\partial t} = -I \frac{\partial^2 y}{\partial x^2} \frac{[\cos\beta - \sin\beta(\partial y/\partial x)]}{[1+(\partial y/\partial x)^2]^{3/2}}, \tag{11}$$

where $I = Ja_p\overline{a}$. Equation (11) describes the leading-order contribution to the evolution of the shape of the ripple from the hopping caused by the saltating particles in the absence of other processes. In the next section, we build upon this picture by including the rolling of the grains under gravity.

B. Rolling

We now incorporate the effect of rolling or avalanching of the sand grains under the influence of gravity. Particles tend to roll down a slope under the influence of gravity balanced by friction [1]. This results in the smoothing of the ripple profile. For a static sand pile, there is an angle of surface slope, known as the angle of repose, which is the maximum that the sand can support before avalanching occurs. The angle of repose depends on the packing of the sand grains, and for dry sand, the angle of repose is about 30° [17]. We assume that for traveling sand ripples, there is an angle γ that is no greater than the angle of repose, and that gives the maximum slope attainable during motion. We will call γ the dynamic angle of repose. If the lee slope increases to the angle γ, then a slip face will develop, on which sand avalanches rather than rolls down the lee slope. This picture is in accord with Bagnold's [1] observation that sand dunes over a certain height have a slip face on the lee slope, and also with Sharp's observation [4] that, near the crest, the lee slopes of sand ripples are straight and inclined roughly at the angle of repose. The slip face is a region extending down from the crest that is maintained at a constant slope γ by avalanching.

As a simple phenomenological model, we assume that for slopes of angle less than γ the grains roll on the surface with speed u, which is a function of the gravitational force along the slope and a coefficient of friction r,

$$u = -\frac{g}{r}\sin\alpha = -\frac{g}{r}\frac{\partial y/\partial x}{[1+(\partial y/\partial x)^2]^{1/2}}. \tag{12}$$

In general r is a function of the grain packing and grain size. In the present work, for simplicity, we set r to be constant. In practice, rolling may cease to occur on very shallow slopes; our model accounts for this in a simple way by assuming that

rolling is proportional to the slope, although this may be refined in the future with more experimental observations. The horizontal number flux $Q(x,t)$ of sand grains is proportional to the horizontal speed of rolling, $u\cos\alpha$,

$$Q(x,t)=-F\,\frac{g}{r}\,\sin\alpha\,\cos\alpha=-F\,\frac{g}{r}\,\frac{\partial y/\partial x}{[1+(\partial y/\partial x)^2]}, \tag{13}$$

where F is a constant of proportionality. If the angle of slope attempts to exceed γ, we assume that avalanching sets in, and the sand flux down the slope becomes very large. We model this phenomenologically by writing

$$Q(x,t)=-F\,\frac{g}{r}\,\tan^2\gamma \times\frac{\partial y/\partial x}{[1+(\partial y/\partial x)^2][\tan^2\gamma-(\partial y/\partial x)^2]^{1/2}}, \tag{14}$$

so that the sand flux becomes infinite as the ripple slope approaches $\pm\tan\gamma$, but also agrees with expression (13) when the slopes are small. The evolution of the surface profile depends on the surface sand flux according to the equation

$$\frac{\partial y}{\partial t}=-a_p\,\frac{\partial Q}{\partial x}, \tag{15}$$

where once again a_p is the mean size of a sand grain. Combining Eqs. (14) and (15), we see that the variation in elevation at any point x on the ripple, due to the process of rolling, is given by

$$\frac{\partial y}{\partial t}=\tilde{D}\,\frac{\partial^2 y}{\partial x^2}, \tag{16}$$

where

$$\hat{D}=F(\tan^4\gamma)a_p\,\frac{g}{r}\,\frac{1-(\partial y/\partial x)^2}{[1+(\partial y/\partial x)^2]^2[\tan^2\gamma-(\partial y/\partial x)^2]^{1/2}}>0. \tag{17}$$

C. The combined model

If we combine the effects of hopping, Eq. (11), and either rolling, Eq. (16), or avalanching, we may find phenomenological equations governing the evolution of the surface of the ripple, $y(x,t)$.

On the stoss slope, the surface elevation evolves according to the equation

$$\frac{\partial y}{\partial t}\,(x,t)=\left(\tilde{D}-\frac{I[\cos\beta-\sin\beta(\partial y/\partial x)]}{[1+(\partial y/\partial x)^2]^{3/2}}\right)\frac{\partial^2 y}{\partial x^2}. \tag{18}$$

On the lee slope, there is a region just beyond the ripple crest, which is shielded from the saltation flux. This is called the shadow zone, and no hopping occurs there (Fig. 1). In the shadow zone, the surface of the ripple evolves owing to rolling or avalanching according to the equation

$$\frac{\partial y}{\partial t}\,(x,t)=\tilde{D}\,\frac{\partial^2 y}{\partial x^2}. \tag{19}$$

Ahead of the shadow zone, the saltation flux can reach the surface once more. In our model we interpret the position where the shadow zone ends as the trailing edge of the stoss slope of the next ripple. Beyond this point the hopping flux can start to build the sand up again.

Since the field observations described in Sec. I suggest that $|\partial y/\partial x|\leqslant\tan\gamma\simeq\tan 30°$, we will assume that $(\partial y/\partial x)^2\ll 1$. In this approximation, Eq. (18) has the form

$$\frac{\partial y}{\partial t}=\left(\frac{D\,\tan^2\gamma}{[\tan^2\gamma-(\partial y/\partial x)^2]^{3/2}}-I\,\cos\beta\right)\frac{\partial^2 y}{\partial x^2}, \tag{20}$$

where $D=Fa_p(g/r)\tan^2\gamma$ is a constant, and Eq. (19) becomes

$$\frac{\partial y}{\partial t}=\left(\frac{D\,\tan^2\gamma}{[\tan^2\gamma-(\partial y/\partial x)^2]^{3/2}}\right)\frac{\partial^2 y}{\partial x^2}. \tag{21}$$

Here terms of $O(\partial y/\partial x)^2$ and higher are neglected, except in the factor $[\tan^2\gamma-(\partial y/\partial x)^2]^{1/2}$, where both terms are of the same order of magnitude.

We now investigate solutions of this model, first considering a horizontal saltation flux, and then extending the analysis to include inclined saltation fluxes.

III. ISOLATED TRAVELING RIPPLE

We will consider the simple model situation in which the saltation flux is horizontal, (i.e., $\beta=0$). Since the lee slope is completely shielded from the horizontal saltation flux, this ripple is isolated. If the hopping due to saltation, which builds up the stoss slope of the ripple, can overcome the rolling of the particles under gravity, which tends to smooth out surface irregularities, i.e., $I>D$, then a ripple will develop [Eq. (18)].

Our model can describe ripples of fixed shape that propagate steadily in the direction of the saltating flux. The shape of the ripple that develops depends upon the intensity of the saltating flux, and the size of the ripple. The stoss face is built up by saltation until the slope becomes so steep that rolling or avalanching downslope prevents further increase. This happens when the diffusion coefficient in Eq. (20) is zero. We then find the shape of the lee slope of the ripple by conservation of sand flux at the ripple crest.

As the saltating flux increases, there will be a larger flux at the crest, and in this case the lee slope at the crest increases in order to allow the sand to roll ahead of the ripple. If the lee slope angle reaches the dynamic angle of repose, $\tan\gamma$, then according to our simple model, avalanching sets in and a slip face develops just ahead of the crest.

The isolated ripple

Using our model equations (20) and (21), we find that a ripple with shape $y(x-ct)$ propagating at steady speed $c>0$ evolves according to the equations

$$-\frac{\partial\hat{y}}{\partial\xi}=\left(\frac{\hat{D}}{[1-(\partial\hat{y}/\partial\xi)^2]^{3/2}}-1\right)\frac{\partial\hat{y}}{\partial\xi^2},\quad \xi<0, \tag{22}$$

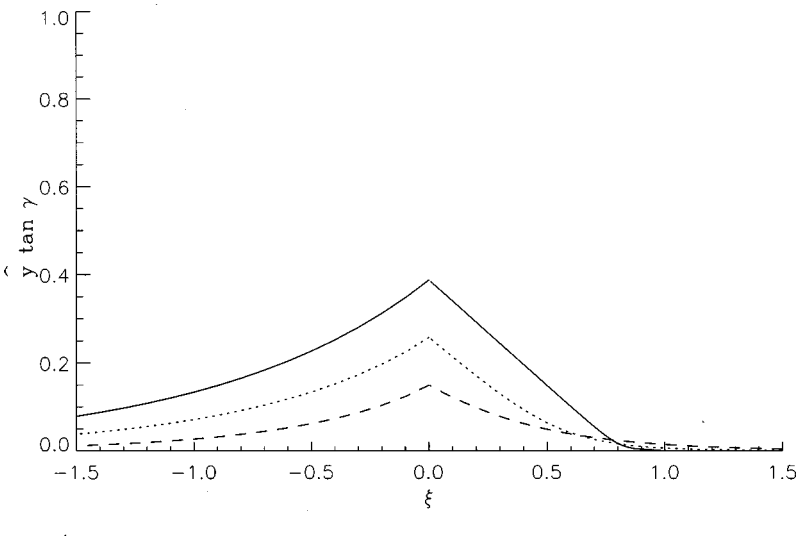

FIG. 2. The shapes of some typical ripples as predicted by our model. The ripple profile, $\hat{y}(\xi)\tan\gamma$ is plotted for $\hat{D}\equiv D/I\tan\gamma=0.05$ (solid curve), 0.20 (dotted curve) and 0.40 (dashed curve). As I increases for fixed D and γ, the ripples grow larger and develop a slip face.

$$-\frac{\partial\hat{y}}{\partial\xi}=\frac{\hat{D}}{[1-(\partial\hat{y}/\partial\xi)^2]^{3/2}}\frac{\partial\hat{y}}{\partial\xi^2},\quad \xi>0, \tag{23}$$

where

$$\xi=\frac{c(x-ct)}{I}, \tag{24}$$

$$\hat{y}=\frac{cy}{I\tan\gamma}, \tag{25}$$

$$\hat{D}=\frac{D}{I\tan\gamma}, \tag{26}$$

and where the ripple crest is at $\xi=0$. Note that both the distance $(x-ct)$ along the ripple, and the ripple height y scale with I/c, so for a given saltation flux intensity, ripples of different speeds are self-similar.

The shape of the lee slope is obtained implicitly by integrating Eq. (23) to give

$$(\hat{D}^2+\hat{y}^2)^{1/2}-\hat{D}=\hat{y}\,\exp\{-(\xi-\xi_0)/\hat{D}-(1+\hat{y}^2/\hat{D}^2)^{1/2}\} \tag{27}$$

on the lee slope, where ξ_0 is a constant that we evaluate below using the boundary conditions that match the lee and stoss sides of the ripple. Note that $y\to 0$ as $\xi\to+\infty$.

The stoss slope of the ripple is built up by saltation until it is so steep that rolling or avalanching of grains balances out the saltation effect. This happens when the effective diffusion coefficient on the stoss slope is zero, i.e.,

$$\frac{\hat{D}}{[1-(\partial\hat{y}/\partial\xi)^2]^{3/2}}=1. \tag{28}$$

At this point, the stoss slope ends at the ripple crest, and there we have

$$\left.\frac{\partial\hat{y}}{\partial\xi}\right|_{0-}=(1-\hat{D}^{2/3})^{1/2}, \tag{29}$$

$$\hat{y}|_0=(1-\hat{D}^{2/3})^{3/2}. \tag{30}$$

Combining Eqs. (27)–(30) we can now determine the constant ξ_0 [Eq. (27)] in terms of $\hat{D}$ from

$$[\hat{D}^2+(1-\hat{D}^{2/3})^3]^{1/2}-\hat{D}=(1-\hat{D}^{2/3})^{3/2}\,\exp\{\xi_0/\hat{D}-[1+(1-\hat{D}^{2/3})^3/\hat{D}^2]^{1/2}\}. \tag{31}$$

From Eq. (22), we find

$$-1=\left(\frac{\hat{D}}{\partial\hat{y}/\partial\xi[1-(\partial\hat{y}/\partial\xi)^2]^{3/2}}-\frac{1}{\partial\hat{y}/\partial\xi}\right)\frac{\partial^2\hat{y}}{\partial\xi^2}, \tag{32}$$

which integrates to give the implicit expression for the gradient of the stoss slope

$$-(\xi-\xi_0)=-(1+\hat{D})\ln\left(\frac{\partial\hat{y}}{\partial\xi}\right)+\frac{\hat{D}}{[1-(\partial\hat{y}/\partial\xi)^2]^{1/2}}+\hat{D}\,\ln\{1-[1-(\partial\hat{y}/\partial\xi)^2]^{1/2}\}. \tag{33}$$

At the crest, the expression on the right-hand side is finite, and this confirms that our model gives a stoss slope of finite extent. The shape of the stoss slope must be determined by numerical integration of Eq. (22), and is shown in Fig. 2.

Matching the sand flux at the crest (and hence the ripple height there, since the ripple is traveling at constant speed) determines the ripple slope on the lee side at the crest. The sand fluxes on the stoss and lee slopes can be deduced from Eqs. (22) and (23), respectively, and are given by

$$\left(\frac{\hat{D}}{[1-(\partial\hat{y}/\partial\xi)^2]^{1/2}}-1\right)\frac{\partial\hat{y}}{\partial\xi}\quad\text{(stoss)}, \tag{34}$$

$$\left(\frac{\hat{D}}{[1-(\partial\hat{y}/\partial\xi)^2]^{1/2}}\right)\frac{\partial\hat{y}}{\partial\xi}\quad\text{(lee)}. \tag{35}$$

Matching the fluxes at the crest we find

$$\left.\frac{\partial\hat{y}}{\partial\xi}\right|_{0+}=\frac{-(1-\hat{D}^{2/3})^{3/2}}{\{\hat{D}^2+(1-\hat{D}^{2/3})^3\}^{1/2}}. \tag{36}$$

We see that as the saltation flux intensity $I \to +\infty$, the rescaled rolling coefficient $\hat{D} \to 0$, and in dimensional form

$$\left.\frac{\partial y}{\partial x}\right|_{0-} \to \tan\gamma, \quad \left.\frac{\partial y}{\partial x}\right|_{0+} \to -\tan\gamma. \tag{37}$$

In particular, the ripple slope at the crest on the lee side tends to the dynamic angle of repose γ and we expect that a slip face will form there.

The height of the ripple varies inversely with the ripple speed, since in dimensional form Eq. (30) gives

$$y|_0 = \frac{I \tan\gamma}{c}\left(1 - \left(\frac{D}{I \tan\gamma}\right)^{2/3}\right)^{3/2}. \tag{38}$$

We deduce that larger ripples travel more slowly than small ripples, at a fixed saltation flux. This naturally causes small ripples to catch up and merge into large ripples, as seen in Sharp's field observations [4], and the numerical simulations of Anderson [3] and Landry and Werner [6].

Note that according to the model, the intensity of the saltation flux must exceed a threshold value, $I > D/\tan\gamma$ ($\hat{D} < 1$), for a ripple to develop. This is in qualitative agreement with the numerical simulations of Nishimori and Ouchi [5]. Bagnold [1] also observed that a threshold wind speed is required for the formation of ripples, but he argued that this is because sand grains require a certain threshold wind speed before they can be brought into saltation. Our prediction results from the assumption that rolling continues on slopes of very small angle, at a rate proportional to the slope. In practice, rolling may cease or become less efficient at very small angles and this might lead to the formation of very small ripples of shallow slope; however, further field observations are necessary to resolve this issue.

The shapes of some typical ripples are shown in Fig. 2. The profiles are very similar to the idealized cross section of a wind ripple, shown in Fig. 7 of Sharp [4], except that here the stoss slope is concave everywhere, while the stoss slope of Sharp's ripple is convex near the crest. Sharp attributes this flattening of the ripple crest to the wind. A possible modification to our model, which might include this effect, would be a treatment of the entrainment of sand grains from the bed by the wind. However, this is beyond the scope of the present work. Note that the model ripples become larger as the saltation flux intensity I increases and $\hat{D}$ decreases below the critical value of 1. For sufficiently large I a slip face develops. The slip face is a region of the lee slope extending down from the crest that is maintained at a constant gradient by avalanching; in our model it increases in length as I increases, since for larger saltation fluxes there is a greater flux of sand at the crest and this is carried rapidly down the ripple by avalanching.

IV. PERIODIC RIPPLE TRAINS: INCLINED SALTATION FLUX

If the saltation flux is not horizontal, but inclined downwards, then the shadow zone becomes of finite extent, and a periodic train of ripples may develop. At the location on the lee slope where the saltation flux once again reaches the surface, the hopping process begins to build up another ripple. In our model, this position will mark the trailing edge of the stoss slope of the next ripple. Hence we can extend our isolated ripple solution to model a train of equally sized ripples propagating steadily with speed c.

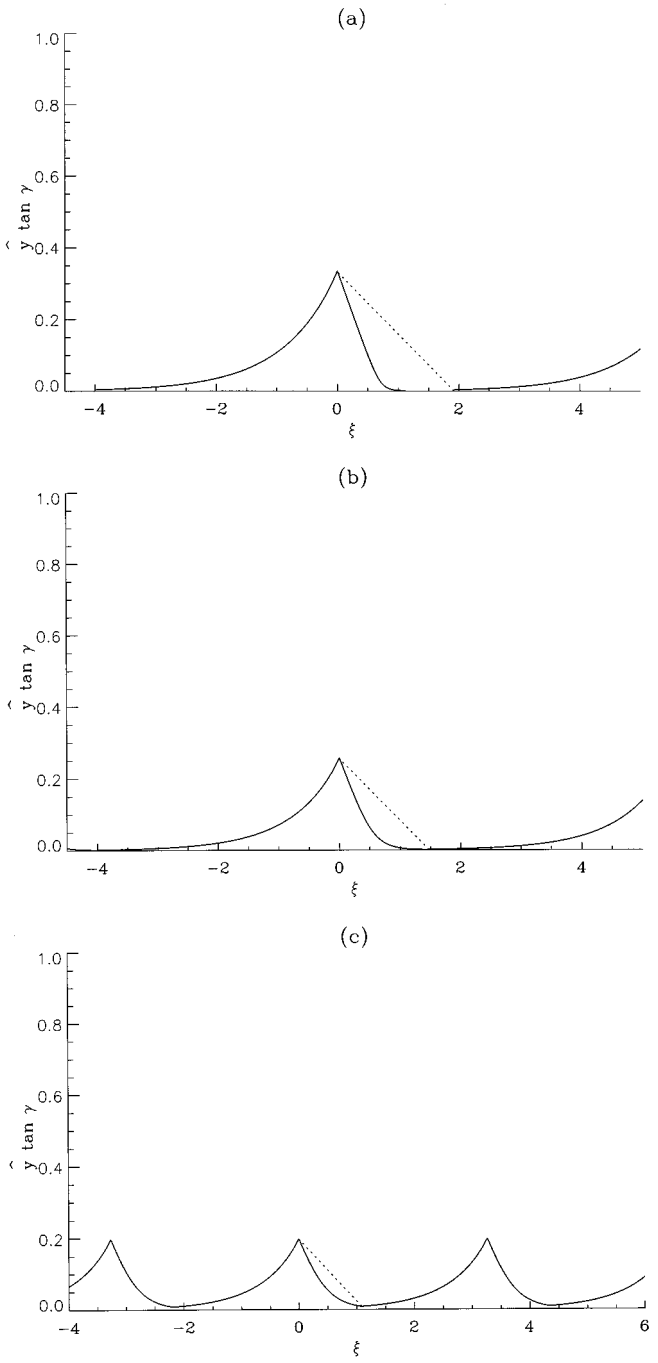

FIG. 3. Typical periodic ripple trains, $\hat{y}(\xi)\tan\gamma$, formed by an inclined saltation flux with $\hat{D} =$ (a) 0.10, (b) 0.20, (c) 0.30. The dotted line indicates the inclination of the saltation flux.

The ripple whose crest is located at $x - ct = 0$ is a modification of the ripple found in Sec. III, with I replaced by $I \cos\beta$, since the angle of inclination of the saltation flux β is now nonzero. The stoss and lee slopes of the ripple are now of finite extent, and occupy the regions $-s \leqslant \xi \leqslant 0$ and $0 \leqslant \xi \leqslant l$, respectively. Typical periodic ripple trains at various values of $\hat{D}$ are shown in Fig. 3.

The model now requires

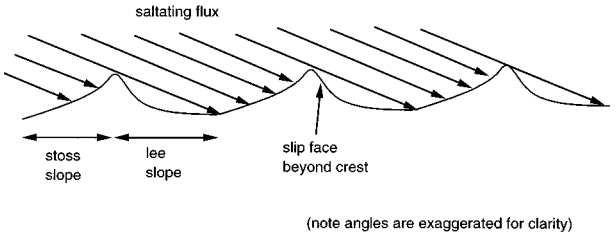

FIG. 4. Diagram of a periodic ripple train, showing the length of the stoss slope s and of the lee slope l, with the coordinate system used in the text, and also showing the position of the slip face.

$$I\cos\beta > D \tag{39}$$

in order for a ripple to develop. Therefore, if the saltation flux is inclined, it must be more intense than in the horizontal case ($\beta=0$) before ripples will form. Bagnold [1] observed that ridges, or isolated ripples, form at lower wind speeds than periodic ripples. He attributed this to the difference in size of the sand grains of which ridges and ripples are composed.

At some point the lee slope emerges from the shadow zone. The location at which this happens is given by $\xi=l$ or $x-ct=l/c$. In our simple model, the lee slope ends where the shadow zone ends; beyond this point the saltating flux builds up a new ripple. Typically, the point at which the lee slope emerges from shadow will not be on the slip face, but on the concave, nearly flat, section of the lee slope, since the inclination of the saltation flux is usually smaller than the dynamic angle of repose, $\beta<\gamma$.

The length l/c of the shadow zone is given by simple geometrical considerations (Fig. 4) and satisfies

$$\left((1-\hat{D}^{2/3})^{3/2}-\frac{l\tan\beta}{\tan\gamma}\right)\exp\left\{-\frac{(l-\xi_0)}{\hat{D}}\right.$$
$$\left.-\left[1+\frac{1}{\hat{D}^2}\left((1-\hat{D}^{2/3})^{3/2}-\frac{l\tan\beta}{\tan\gamma}\right)^2\right]^{1/2}\right\}$$
$$=\left[\hat{D}^2+\left((1-\hat{D}^{2/3})^{3/2}-\frac{l\tan\beta}{\tan\gamma}\right)^2\right]^{1/2}-\hat{D}. \tag{40}$$

We see that l can be expressed in terms of $\hat{D}$ and the angles β and γ. So for fixed D, I, β, and γ, the length l/c of the shadow zone varies inversely with the ripple speed c and hence is directly proportional to the ripple height, so that taller ripples have longer shadow zones.

At $x-ct=l$, another ripple starts to grow. If the ripples are periodic, so that they are the same shape and all have the same amplitude, then the ripple will have its crest at a position $\xi=\lambda=l+s$, $x-ct=(l+s)/c$. Continuity of surface elevation and sand flux at $\xi=l$ requires that

$$\hat{y}(l)=\hat{y}(-s). \tag{41}$$

Since the shape of the stoss slope is found from a numerical integration of Eq. (22), this matching must also be performed numerically. From Fig. 3 we note that since the saltation flux is inclined at a very shallow angle to the horizontal (5°–10°), the ripple height at the end of the lee slope or beginning of the stoss slope is very small. The shadow zone is therefore long in comparison with the lee slope decay length scale, and dominates the ripple wavelength, corroborating Sharp's argument [4] that the ripple wavelength is controlled by the length of the shadow region. Note also that simply from geometrical considerations, taller ripples have a longer shadow zone, and hence a longer wavelength. This is in accord with field observations (e.g., Cornish [13]), which have established that sand ripples have aspect ratios in the relatively narrow range 1/15–1/20. Note also that for a fixed ripple height, as the angle of inclination of the saltation flux β increases, the wavelength λ decreases, so the ripples become closer together.

Replacing I by $I\cos\beta$ in Eq. (38) we find that for the periodic train the ripple height is related to the speed by

$$y|_0=\frac{I\cos\beta\tan\gamma}{c}\left[1-\left(\frac{D}{I\cos\beta\tan\gamma}\right)^{2/3}\right]^{3/2}. \tag{42}$$

Just as in the case of a horizontal saltation flux, smaller ripples travel faster than larger ones, providing a mechanism for the cascade to progressively larger ripples with time, as shorter ripples catch up with and are incorporated into larger ones.

V. CONCLUSION

In this work, we have formulated a simple phenomenological model of sand ripple migration based on a balance between grain hopping driven by saltation and rolling or avalanching under gravity. We have found solutions describing steadily propagating isolated ripples, produced by a horizontal saltation flux, and periodic trains of ripples, which develop when the saltation flux is inclined to the horizontal. In the case of an inclined saltation flux, we show that the ripple wavelength is controlled by the length of the shadow zone, as suggested by Sharp [4]. Although very simple, our model predicts some of the qualitative features shown by sand ripples in experimental or field studies [1,4].

Our model incorporates Bagnold's [1] observation that saltation is responsible for the development of aeolian sand ripples, and we find that ripples only develop if there is a sufficiently intense saltating flux ($I>D$), so that grains can accumulate by hopping under saltation faster than they can return to their original position through rolling under gravity. We note, however, that if, in practice, rolling becomes ineffective on slopes of very small angle, then very small ripples may still develop as a result of saltation. Our model also predicts that at relatively low saltation fluxes, the lee slope of the ripple is a smooth curve, but that as the saltation flux increases, a slip face develops near the crest.

In contrast to Sharp's [4] conjecture that ripples become more symmetric as wind speed increases, our model ripples tend to look more asymmetric as the saltation flux intensity I increases in the non-slip-face regime. Once a slip face has developed, however, its length increases with increasing I leading the ripples to become more symmetrical again. Our model is very simple, and it is likely that more complex effects such as wind entrainment of sand have an effect on ripple symmetry.

The model predicts a decrease in the speed of propagation

as the ripple becomes larger, essentially since more time is required for the grains to hop the length of the ripple. This is consistent with Sharp's observation [4] that smaller ripples are eliminated by ripple merger, and with Anderson's [3] and Landry and Werner's [6] numerical simulations where small ripples catch up with and may become incorporated into larger, slower moving ripples.

For periodic trains of equally sized, steadily propagating ripples, the model predicts that larger, slower moving waves will have longer wavelengths in accordance with observation [13]. In addition we find that the spacing between the waves decreases as the impact angle of the saltation flux increases.

In our model we have only considered a simple situation in which the shape and speed of the ripple are based solely upon the local dynamical balance between hopping and rolling or slipping. As described above, our model appears to capture many of the qualitative aspects of the motion of aeolian sand ripples. However, in some real situations, other effects may also be important in determining the shape and size of ripples. These include the effects of multiple grain sizes, which may lead to more complex hopping phenomena [15], and the effects of the deposition and entrainment of grains by wind, which is responsible for the formation of the saltation flux. In particular, it would be interesting to couple the present model with a model of the generation of the saltation flux by wind entrainment.

[1] R. A. Bagnold, *The Physics of Blown Sand and Desert Dunes* (Methuen and Co., London, 1941).
[2] R. S. Anderson, Sedimentology **34**, 943 (1987).
[3] R. S. Anderson, Earth-Sci. Rev. **29**, 77 (1990).
[4] R. P. Sharp, J. Geol. **71**, 617 (1963).
[5] H. Nishimori and N. Ouchi, Int. J. Mod. Phys. B **7**, 2025 (1993); Phys. Rev. Lett. **71**, 197 (1993).
[6] W. Landry and B. T. Werner, Physica D **77**, 238 (1994).
[7] J. Ungar and P. K. Haff, Sedimentology **34**, 289 (1987).
[8] S. Mitha, M. Q. Tran, B. T. Werner, and P. K. Haff, Acta Mech. **63**, 267 (1986).
[9] R. E. Hunter, Sedimentology **32**, 409 (1985).
[10] R. S. Anderson, Sedimentology **35**, 175 (1988).
[11] D. A. Rumpel, Sedimentology **32**, 267 (1985).
[12] K. Pye and H. Tsoar, *Aeolian Sand and Sand Dunes* (Unwin Hyman, London, 1990).
[13] V. Cornish, *Waves of Sand and Snow* (T. Fisher Unwin, London, 1914).
[14] S. B. Forrest and P. K. Haff, Science **255**, 1240 (1992).
[15] R. S. Anderson and K. L. Bunas, Nature (London) **365**, 740 (1993).
[16] R. B. Hoyle (unpublished).
[17] A. von Burkalow, Bull. Geol. Soc. Am. **56**, 669 (1945).